CAT: Compression-Aware Training for bandwidth reduction

Anonymous authors
Paper under double-blind review

Abstract

Convolutional neural networks (CNNs) have become the dominant neural network architecture for solving visual processing tasks. One of the major obstacles hindering the ubiquitous use of CNNs for inference is their relatively high memory bandwidth requirements, which can be a main energy consumer and throughput bottleneck in hardware accelerators. Accordingly, an efficient feature map compression method can result in substantial performance gains. Inspired by *quantization-aware training* approaches, we propose a compression-aware training (CAT) method that involves training the model in a way that allows better compression of feature maps during inference. Our method trains the model to achieve low-entropy feature maps, which enables efficient compression at inference time using classical transform coding methods. CAT significantly improves the state-of-the-art results reported for quantization. For example, on ResNet-34 we achieve 73.1% accuracy (0.2% degradation from the baseline) with an average representation of only 1.79 bits per value. Reference implementation accompanies the paper.

1 Introduction

Deep Neural Networks (DNNs) have become a popular choice for a wide range of applications such as computer vision, natural language processing, autonomous cars, etc. Unfortunately, their vast demands for computational resources often prevents their use on power-challenged platforms. The desire for reduced bandwidth and compute requirements of deep learning models has driven research into quantization (Hubara et al., 2016; Yang et al., 2019b; Liu et al., 2019; Gong et al., 2019), pruning (LeCun et al., 1990; Li et al., 2017; Molchanov et al., 2019), and sparsification (Gale et al., 2019; Dettmers & Zettlemoyer, 2019).

In particular, quantization works usually focus on scalar quantization of the feature maps: mapping the activation values to a discrete set $\{q_i\}$ of size L. Such a representation, while being less precise, is especially useful in custom hardware, where it allows more efficient computations and reduces the memory bandwidth. In this work, we focus on the latter, which has been shown to dominate the energy footprint of CNN inference on custom hardware (Yang et al., 2017). We show that the quantized activation values $\{q_i\}$ can further be coded to reduce memory requirements.

The raw quantized data require $\lceil \log_2(L) \rceil$ bits per value for storage. This number can be reduced by compressing the feature maps. In particular, in the case of element-wise compression of independent identically distributed values, the lower bound of amount of bits per element is given by the entropy

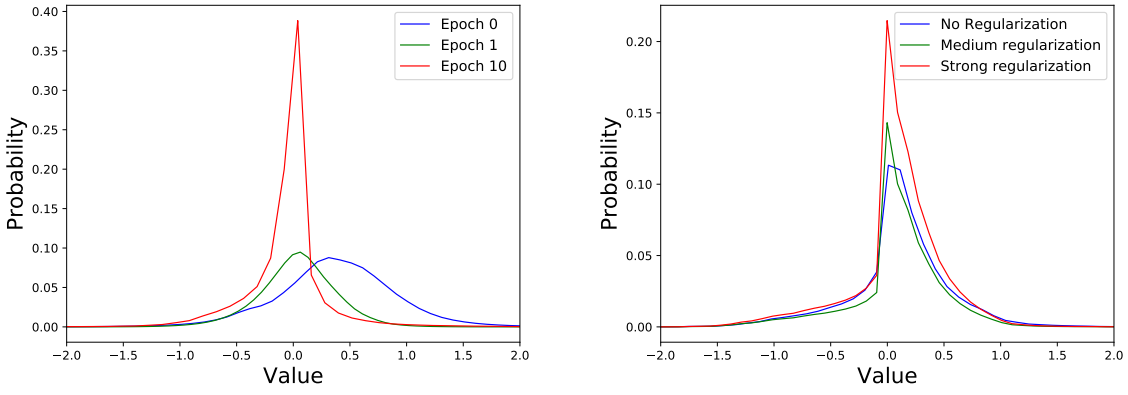

(a) (b)

Figure 1: Pre-activation distributions of one layer in ResNet-18. **(a) Evolution at different epochs.** As training progresses, the probability of non-positive pre-activation values increases, zeroing more post-ReLU values. The sharp peak at zero reduces entropy and thus improves compressibility. **(b) Effect of entropy regularization.** Without regularization, the distribution has much heavier tails and thus has higher entropy. With increasing regularization, the probability of extreme values is significantly reduced. The entropy penalty λ was selected so that the overall accuracy is not affected. The compression ratio in the strongly regularized case is 2.23 higher compared to the unregularized the baseline.

(Shannon, 1948):

$$H(\mathbf{q}) = -\sum_{i=1}^{L} p(q_i) \log_2 p(q_i) \tag{1}$$

of the quantized values $\{q_i\}$, where $p(q_i)$ denotes the probability of q_i.

In this work, we take a further step by manipulating the distribution of the quantization values so that the entropy $H(q)$ is minimized. To that end, we formulate the training problem by augmenting the regular task-specific loss (the cross-entropy classifier loss in our case) with the feature map entropy serving as a proxy to the memory rate. The strength of the latter penalty is controlled through a parameter $\lambda > 0$. Fig. 1 demonstrates the effect of the entropy penalty on the compressibility of the intermediate activations.

Contributions. Our paper makes several contributions. Firstly, we introduce Compression-Aware Training (CAT), a technique for memory bandwidth reduction. The method works by introducing a loss term that penalizes the entropy of the activations at training time and applying entropy encoding (e.g., Huffman coding) on the resulting activations at inference time. Since the only overhead of the method at inference time is entropy encoding that can be implemented efficiently, the improvement is universal for any hardware implementation, being especially efficient on computationally optimized ones, where memory I/O dominates the energy footprint (Yang et al., 2017; Jouppi et al., 2017). We demonstrate a 2 to 4-fold memory bandwidth reduction for multiple architectures: MobileNetV2 and ResNet on the ImageNet visual recongition task, and SSD512 on the PASCAL VOC object

detection task. We also investigate several differentiable loss functions which lead to activation entropy minimization and show a few alternatives that lead to the same effect.

Finally, we analyze the rate-distortion tradeoff of the method, achieving even stronger compression at the expense of minor accuracy reduction: for ResNet-18, we manage to achieve entropy inferior to one bit per value, at the expense of losing 2% of the top-1 accuracy.

2 Related work

Recent studies (Yang et al., 2017; Wang et al., 2019) have shown that almost 70% of the energy footprint on custom hardware is due to the data movement to and from the off-chip memory. Nonetheless, the techniques for memory bandwidth reduction have not yet received significant attention in the literature. One way to improve memory performance is by fusing convolutional layers Xiao et al. (2017), Xing et al. (2019), reducing the number of feature maps transfers. This reduces both runtime and energy consumption of the hardware accelerator. Another option is to use on-chip cache instead of external memory. Morcel et al. (2019) have shown order of magnitude improvement in power consuption using this technique. Another important system parameter dominated by the memory bandwidth is latency. Jouppi et al. (2017) and Wang et al. (2019) showed that the state-of-the-art DNN accelerators are memory-bound, implying that increasing computation throughput without reducing the memory bandwidth barely affects the total system latency.

Quantization reduces computation and memory requirements; 16-bit fixed point has become a *de facto* standard for fast inference. In most applications, weights and activations can be quantized down to 8 bits without noticeable loss of precision (Lee et al., 2018; Yang et al., 2019a). Further quantization to lower precision requires non-trivial techniques (Mishra et al., 2018; Zhang et al., 2018), which are currently capable of reaching around $3-4$ without compromising precision (Choi et al., 2018b;a; Dong et al., 2019).

Another way to reduce memory bandwidth is by compressing the intermediate activations prior to their transfer to memory with some computationally cheap encoding, such that Huffman (Chandra, 2018; Chmiel et al., 2019) or run-length (RLE) encoding (Cavigelli et al., 2019). A similar approach of storing only nonzero values was utilized by Lin & Lai (2018). (Chmiel et al., 2019) used linear dimensionality reduction (PCA) to increase the effectiveness of Huffman coding, while Gudovskiy et al. (2018) proposed to use nonlinear dimensionality reduction techniques.

Lossless coding was previously utilized in a number of ways for DNN compression: Han et al. (2016) and Zhao et al. (2019) used Huffman coding to compress weights, while Wijayanto et al. (2019) used more complicated DEFLATE (LZ77 + Huffman) algorithm for the same purpose. Aytekin et al. (2019) proposed to use compressibility loss, which induces sparsity and has been shown (empirically) to reduce entropy of the non-zero part of the activations.

3 Method

We consider a feed-forward DNN $\mathcal{F}$ composed of L layers; each subsequent layer processing the output of the previous one: $x^i = \mathcal{F}_i\left(x^{i-1}\right)$, using the parameters $\mathbf{w} \in \mathbb{R}^N$. We denote by $x^0 = x$ and $x^L = y$ the input and the output of the network, respectively.

The parameters $\mathbf{w}$ of the network are learned by minimizing $\mathcal{L}(x, y; \mathbf{w}) + \lambda\mathcal{R}(\mathbf{w})$, with the former term $\mathcal{L}$ being the task loss, and the latter term $\mathcal{R}$ being a regularizer (e.g., $\|\mathbf{w}\|_2$) inducing some properties on the parameters $\mathbf{w}$.

3.1 Entropy encoding and rate regularization

Entropy encoders are a family of lossless data encoders which compress each symbol independently. In this case, assuming i.i.d. distribution of the input, it has been show that optimal code length is $-\log_b p$, where b is number of symbols and p_i is the probability of i$^{\text{th}}$ symbol (Shannon, 1948). Thus, for a discrete random variable X we define an entropy $H(X) = -\mathbb{E}\log_2 X = -\sum_i p(x_i)\log_2 p(x_i)$, which is a lower bound of the amount of information required for lossless compression of X. The expected total space required to encode the message is $N \cdot H$, where N is number of symbols. Since we encode the activations with entropy encoder before writing them into memory, we would like to minimize the entropy of the activations to improve the compression rate.

One example of entropy encoder is Huffman coding – a prefix coding which assigns shorter codes to the more probable symbols. It is popular because of simplicity along with high compression rate (Szpankowski, 2000) bounded by $H(X) \leq R \leq H(X)+1$ (the comparison of Huffman coding rates to entropy is shown in Fig. 3). Another entropy encoder is arithmetic coding – highly efficient encoder which achieves optimal rates for big enough input but requires more computational resources for encoding.

3.2 Differentiable entropy-reducing loss

Since the empirical entropy is a discrete function, it is not differentiable and thus cannot be directly minimized with gradient descent. Nevertheless, there exist a number of differentiable functions which either approximate entropy or have same minimizer. Thus we optimize

$$\mathcal{L} = \mathcal{L}_{\text{p}} + \lambda\mathcal{L}_H, \tag{2}$$

where $\mathcal{L}_{\text{p}}$ is a target loss function and $\mathcal{L}_H$ is some regularization which minimizes entropy.

Soft entropy First, we consider the differentiable entropy estimation suggested by Agustsson et al. (2017). Ws start from definition of the entropy,

$$H(X) = -\sum p(x_i)\log(p(x_i)) \tag{3}$$

$$p_i = \frac{|\{x|x = q_i\}|}{N}, \tag{4}$$

where $\mathbf{q}$ is a vector of quantized values. Let m be an index of the bin the current value is mapped to, and $\mathbf{Q}$ a one-hot encoding of this index, i.e.,

$$q_m = \arg\min_{q_i \in \mathcal{Q}} |x - q_i| = \arg\max_{q_i \in \mathcal{Q}} (-|x - q_i|) \tag{5}$$

$$\mathbf{Q}_i = \delta_{im}, \tag{6}$$

where δ_{im} denotes Kroneker's delta. To make the latter expression differentiable, we can replace argmax with softmax:

$$\tilde{\mathbf{Q}}(x) = \text{softmax}(-|\mathbf{x} - \mathbf{q}|, T), \tag{7}$$

where T is the temperature parameter, and $\tilde{Q}(x) \to Q(x)$ as $T \to \infty$.

Finally, the soft entropy $\hat{H}$ is defined as

$$\hat{p}_i = \frac{\sum_j \tilde{\mathbf{Q}}_i(x_j)}{N} \tag{8}$$

$$\hat{H}(X) = -\sum \hat{p}(x_i) \log(\hat{p}(x_i)) \tag{9}$$

To improve both memory requirements and time complexity of the training, we calculate soft entropy only on part of the batch, reducing the amount of computation and the gradient tensor size.

Compressibility loss for entropy reduction An alternative loss promoting entropy reduction was proposed by Aytekin et al. (2019) under the name of *compressibility loss* and based on earlier work by Hoyer (2004):

$$\mathcal{L}_c = \frac{\|\mathbf{x}\|_1}{\|\mathbf{x}\|_2} \tag{10}$$

This loss has the advantage of computational simplicity, and has been shown both theoretically and practically to promote sparsity and low entropy in input vectors. While originally applied to the weights of the network, here we apply the same loss to the activations.

As shown in Section 4.1, both the soft entropy and the compressibility loss lead to similar results.

Our method for reducing memory bandwidth can be described as follows: at training time, we fine-tune (training from scratch should also be possible, but we have not tested it) the pre-trained network $\mathcal{F}$ with the regularized loss (2), where we use $\mathcal{L}_H = \sum \hat{H}(x_i)$ in case of differentiable entropy and $\mathcal{L}_H = \sum \mathcal{L}_c(x_i)$ in case of compressability loss. At test time, we apply entropy coding on the activations before writing them to memory, thus reducing the amount of memory transactions. In contrast to Chmiel et al. (2019), who avoided fine-tuning by using test time transformation in order to reduce entropy, our method does not requires complex transformations at test time by inducing low entropy during training.

4 Experimental Results

We evaluate the proposed scheme on common CNN architectures for image classification on ImageNet (ResNet-18/34/50, MobileNetV2), and object detection on Pascal VOC dataset (SSD512[1] (Liu et al., 2016)). The weights were initialized with pre-trained model and quantized with uniform quantization using the shadow weights, i.e. applying updates to a full precision copy of quantized weights (Hubara et al., 2016; Rastegari et al., 2016). The activation were clipped with a learnable parameter and then uniform quantized as suggested by Baskin et al. (2018). Similarly to previous works (Zhou et al., 2016; Rastegari et al., 2016), we used the straight-through estimator (Bengio et al., 2013) to approximate the gradients. We quantize all layers in the network, in contrast to the common practice of leaving first and last layer in high-precision (Zhou et al., 2016; Baskin et al., 2018). Since the weights are quantized only to 8 bit, we have noticed small to no difference between the quantized and non-quantized weights.

For optimization, we use SGD with a learning rate of 10^{-4}, momentum 0.9, and weight decay 4×10^{-5} for up to 30 epochs (usually, $10 - 15$ epochs were sufficient for convergence). Our initial

[1]Our code is based on implementation by Li (2018).

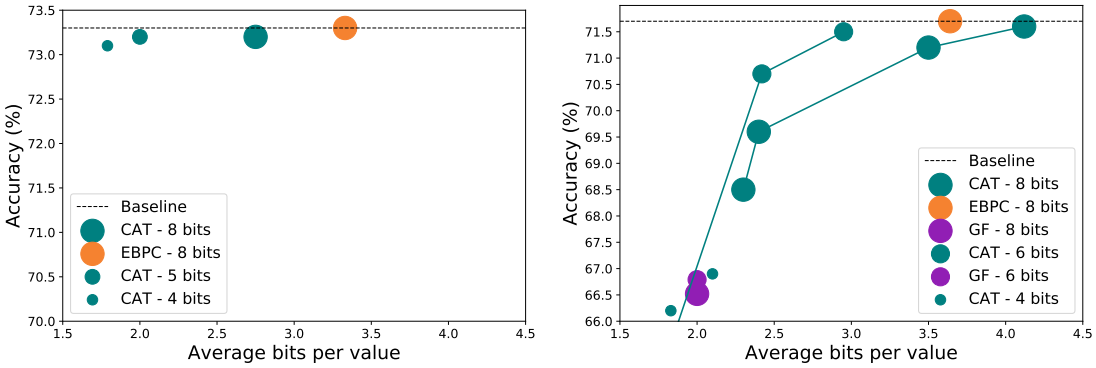

(a) (b)

Figure 2: Comparison with other methods: EPBC (Cavigelli et al. (2019)) and GF (Gudovskiy et al. (2018)) in **(a) ResNet-34** and **(b) MobilenetV2**. Different marker size refers to different activation bitwidths before compression. For GF, compression rate was averaged only over compressed layers.

Table 1: Results for ResNet-18, ResNet-50, and SSD512. For comparison we include the results obtained by Gudovskiy et al. (2018) for the SSD512 model on the same task but with a different backbone, for which we obtain a better compression rate with a lower accuracy degradation. Compute denotes activation bitwidth used for arithmetic operations. Memory denotes average number of bits for memory transactions (after compression). Compression ratio denotes the reduction in representation size. Weight bitwidth is 8 except the full-precision experiments. Additional experimental results are provided in Appendix A.

Architecture	**Compute (bits)**	**Memory (bits)**	**Compression ratio**	**Top-1 accuracy (%)**
ResNet-18, CAT	32	32	1	69.70
	5	1.5	3.33	69.20
	4	1.51	2.65	68.08
ResNet-50, CAT	32	32	1	76.1
	5	1.60	3.125	74.90
	4	1.78	2.25	74.50
SSD512-SqueezeNet (Gudovskiy et al., 2018)	32	32	1	68.12
	8	2	4	64.39
	6	2	3	62.09
SSD512-VGG, CAT	32	32	1	80.72
	6	2.334	2.57	77.49
	4	1.562	2.56	77.43

choice of temperature was $T = 10$, which performed well. We tried, following the common approach (Jang et al., 2016), to apply exponential scheduling to the temperature, but it did not have any noticeable effect on the results.

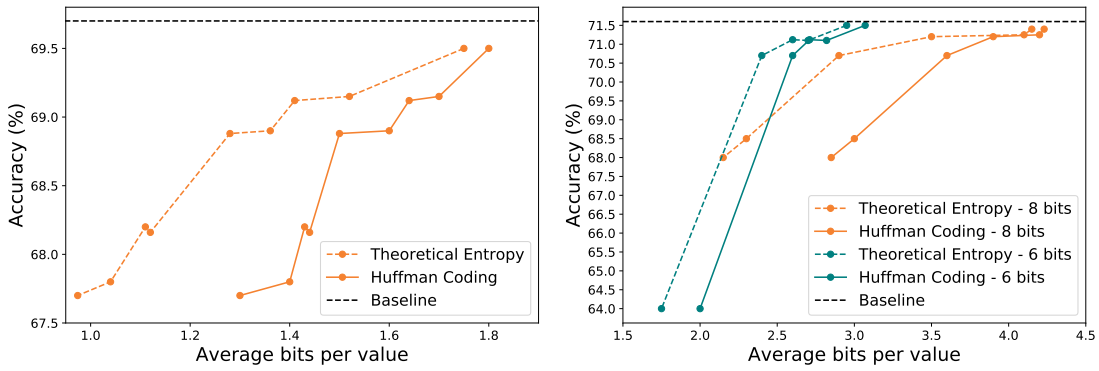

(a) (b)

Figure 3: Tradeoff between rate and accuracy for different values of λ (ranged between 0 and 0.3) in **(a) ResNet-18** and **(b) MobileNetV2**. In ResNet-18 the activations are quantized to 5 bits, in MobileNet we show results for activation quantized to 6 and 8 bits.

In Fig. 2 we compare our method with EPBC (Cavigelli et al. (2019)) and GF (Gudovskiy et al. (2018)). EPBC is based on a lossless compression method that maintains the full precision accuracy while reducing bit rate to approximately 3.5 bits/value in both models. GF, on the other hand, provides strong compression at the expense of larger accuracy degradations. In addition, Gudovskiy et al. (2018) have compressed only part of the layers. Unlike these two methods, CAT allows more flexible tradeoff between compression and accuracy. CAT shows better results in ResNet-34 and show either better accuracy or compression for MobileNetV2. We also run our method on additional architectures: ResNet-18, ResNet-50, and SSD512 with VGG backbone; the results are listed in Table 1. Even though we can not directly compare detection results with Gudovskiy et al. (2018), the drop in accuracy is lower in our case.

4.1 Ablation study

Rate-Accuracy Tradeoff The proposed CAT algorithm tries to balance between minimizing the rate and maximizing the accuracy of the network by means of the parameter λ in Eq. (2). To check this tradeoff, we run the same experiment in ResNet-18 and MobileNetV2 with different values of λ in the range of $0 - 0.3$, with results shown in Fig. 3. We show the results of the theoretical entropy and of the Huffman coding, which was chosen for its simplicity but more efficient encoders can be combined with our method. For higher rate Huffman coding is close ($\sim$3% overhead) to the theoretical entropy, while for lower entropy the difference is higher and is bounded by 1 bit per value – in the latter case, different lossless coding schemes such as arithmetic coding can provide better results.

Robustness For checking the robustness of our method, we performed several runs with the same hyper-parameters and a different random seed. Statistics reported in Table 2 suggest that the method is robust and stable under random intialization.

Soft entropy vs. compressibility loss Replacing the soft entropy with a different loss which minimizes the entropy almost did not affect the results, as shown in Table 3. We conclude that

Table 2: Mean and standard deviation over multiple runs of ResNet-18 and ResNet-34.

Architecture	**Compute, bits**	**Runs**	**Accuracy, % (mean±std)**	**Memory, bits (mean±std)**
ResNet-18	5	5	69.122±0.016	1.5150±0.0087
ResNet-34	5	4	73.025±0.095	1.7875±0.033

Table 3: Performance of soft entropy (9) and compressibility loss (10) on ResNet-18.

Compute, bits	**Loss**	**Accuracy**	**Memory, bits**
4	entropy	67.86%	1.43
4	compressability	67.84%	1.50
5	entropy	69.49%	1.79
5	compressability	69.36%	1.73

the desired effect is a result of entropy reduction rather than a particular form of regularization promoting it.

Batch size We have noticed that training ResNet-50 on a single GPU mandated the use of small batches, leading to performance degradation. Increasing the batch size from 16 to 64 without changing other hyperparameters increased accuracy by more than 0.5% with entropy increase by less than 0.1 bits/value.

5 Discussion

Quantization of activations reduces memory access costs which are responsible for a significant part of energy footprint in NN accelerators. Conservative quantization approaches, known as post-training quantization, take a model trained for full precision and directly quantize it to 8-bit precision. These methods are simple to use and allow for quantization with limited data. Unfortunately, post-training quantization below 8 bits usually incurs significant accuracy degradation. Quantization-aware training approaches involve some sort of training either from scratch (Hubara et al., 2016), or as a fine-tuning step from a pre-trained floating point model (Han et al., 2016). Training usually compensates significantly for model's accuracy loss due to quantization.

In this work, we take a further step and propose a compression-aware training method to aggressively compress activations to as low as 2 average bit/value representations without harming accuracy. Our method optimizes the average-bit per value needed to represent activation values by minimizing the entropy. We demonstrate the applicability of our approach on classification tasks using the models MobileNetV2, ResNet, and object detection task using the model SSD512. Due to the low overhead, the method provides universal improvement for any custom hardware, being especially useful for the accelerators with efficient computations, where memory transfers are a significant part of the energy budget. We show that the effect is universal among loss functions and robust to random initialization.

References

Eirikur Agustsson, Fabian Mentzer, Michael Tschannen, Lukas Cavigelli, Radu Timofte, Luca Benini, and Luc V. Gool. Soft-to-hard vector quantization for end-to-end learning compressible representations. In I. Guyon, U. V. Luxburg, S. Bengio, H. Wallach, R. Fergus, S. Vishwanathan, and R. Garnett (eds.), *Advances in Neural Information Processing Systems 30*, pp. 1141–1151. Curran Associates, Inc., 2017. URL http://papers.nips.cc/paper/6714-soft-to-hard-vector-quantization-for-end-to-end-learning-compressible-representations.pdf. (cited on p. 4)

Caglar Aytekin, Francesco Cricri, and Emre Aksu. Compressibility loss for neural network weights. *arXiv preprint arXiv:1905.01044*, 2019. URL http://arxiv.org/abs/1905.01044. (cited on pp. 3 and 5)

Chaim Baskin, Natan Liss, Yoav Chai, Evgenii Zheltonozhskii, Eli Schwartz, Raja Giryes, Avi Mendelson, and Alexander M. Bronstein. NICE: noise injection and clamping estimation for neural network quantization. *CoRR*, abs/1810.00162, 2018. URL http://arxiv.org/abs/1810.00162. (cited on p. 5)

Yoshua Bengio, Nicholas Léonard, and Aaron C. Courville. Estimating or propagating gradients through stochastic neurons for conditional computation. *CoRR*, abs/1308.3432, 2013. URL http://arxiv.org/abs/1308.3432. (cited on p. 5)

Lukas Cavigelli, Georg Rutishauser, and Luca Benini. EBPC: Extended bit-plane compression for deep neural network inference and training accelerators. *arXiv preprint arXiv:1908.11645*, 2019. (cited on pp. 3, 6, and 7)

Mahesh Chandra. Data bandwidth reduction in deep neural network socs using history buffer and huffman coding. In *2018 International Conference on Computing, Power and Communication Technologies (GUCON)*, pp. 1–3. IEEE, 2018. (cited on p. 3)

Brian Chmiel, Chaim Baskin, Ron Banner, Evgenii Zheltonozhskii, Yevgeny Yermolin, Alex Karbachevsky, Alex M. Bronstein, and Avi Mendelson. Feature map transform coding for energy-efficient cnn inference. *arXiv preprint arXiv:1905.10830*, May 2019. URL http://arxiv.org/abs/1905.10830. (cited on pp. 3 and 5)

Jungwook Choi, Pierce I-Jen Chuang, Zhuo Wang, Swagath Venkataramani, Vijayalakshmi Srinivasan, and Kailash Gopalakrishnan. Bridging the accuracy gap for 2-bit quantized neural networks (qnn). *arXiv preprint arXiv:1807.06964*, 2018a. URL https://arxiv.org/abs/1807.06964. (cited on p. 3)

Jungwook Choi, Zhuo Wang, Swagath Venkataramani, Pierce I-Jen Chuang, Vijayalakshmi Srinivasan, and Kailash Gopalakrishnan. Pact: Parameterized clipping activation for quantized neural networks. *arXiv preprint arXiv:1805.06085*, 2018b. (cited on p. 3)

Tim Dettmers and Luke Zettlemoyer. Sparse networks from scratch: Faster training without losing performance. *arXiv preprint arXiv:1907.04840*, 2019. URL https://arxiv.org/abs/1907.04840. (cited on p. 1)

Zhen Dong, Zhewei Yao, Amir Gholami, Michael Mahoney, and Kurt Keutzer. Hawq: Hessian aware quantization of neural networks with mixed-precision. *arXiv preprint arXiv:1905.03696*, 2019. (cited on p. 3)

Trevor Gale, Erich Elsen, and Sara Hooker. The state of sparsity in deep neural networks. *arXiv preprint arXiv:1902.09574*, 2019. URL https://arxiv.org/abs/1902.09574. (cited on p. 1)

Ruihao Gong, Xianglong Liu, Shenghu Jiang, Tianxiang Li, Peng Hu, Jiazhen Lin, Fengwei Yu, and Junjie Yan. Differentiable soft quantization: Bridging full-precision and low-bit neural networks. *arXiv preprint arXiv:1908.05033*, 2019. URL http://arxiv.org/abs/1908.05033. (cited on p. 1)

Denis Gudovskiy, Alec Hodgkinson, and Luca Rigazio. Dnn feature map compression using learned representation over gf(2). In *The European Conference on Computer Vision (ECCV) Workshops*, September 2018. (cited on pp. 3, 6, and 7)

Song Han, Huizi Mao, and William J Dally. Deep compression: Compressing deep neural networks with pruning, trained quantization and huffman coding. *International Conference on Learning Representations (ICLR)*, 2016. (cited on pp. 3 and 8)

Patrik O. Hoyer. Non-negative matrix factorization with sparseness constraints. *Journal of machine learning research*, 5(Nov):1457–1469, 2004. URL http://www.jmlr.org/papers/v5/hoyer04a.html. (cited on p. 5)

Itay Hubara, Matthieu Courbariaux, Daniel Soudry, Ran El-Yaniv, and Yoshua Bengio. Quantized neural networks: Training neural networks with low precision weights and activations. *arXiv preprint arXiv:1609.07061*, 2016. URL https://arxiv.org/abs/1609.07061. (cited on pp. 1, 5, and 8)

Eric Jang, Shixiang Gu, and Ben Poole. Categorical reparameterization with gumbel-softmax. *arXiv preprint arXiv:1611.01144*, 2016. URL https://arxiv.org/abs/1611.01144. (cited on p. 6)

Norman P. Jouppi, Cliff Young, Nishant Patil, David A. Patterson, Gaurav Agrawal, Raminder Bajwa, Sarah Bates, Suresh Bhatia, Nan Boden, Al Borchers, Rick Boyle, Pierre-luc Cantin, Clifford Chao, Chris Clark, Jeremy Coriell, Mike Daley, Matt Dau, Jeffrey Dean, Ben Gelb, Tara Vazir Ghaemmaghami, Rajendra Gottipati, William Gulland, Robert Hagmann, Richard C. Ho, Doug Hogberg, John Hu, Robert Hundt, Dan Hurt, Julian Ibarz, Aaron Jaffey, Alek Jaworski, Alexander Kaplan, Harshit Khaitan, Andy Koch, Naveen Kumar, Steve Lacy, James Laudon, James Law, Diemthu Le, Chris Leary, Zhuyuan Liu, Kyle Lucke, Alan Lundin, Gordon MacKean, Adriana Maggiore, Maire Mahony, Kieran Miller, Rahul Nagarajan, Ravi Narayanaswami, Ray Ni, Kathy Nix, Thomas Norrie, Mark Omernick, Narayana Penukonda, Andy Phelps, Jonathan Ross, Amir Salek, Emad Samadiani, Chris Severn, Gregory Sizikov, Matthew Snelham, Jed Souter, Dan Steinberg, Andy Swing, Mercedes Tan, Gregory Thorson, Bo Tian, Horia Toma, Erick Tuttle, Vijay Vasudevan, Richard Walter, Walter Wang, Eric Wilcox, and Doe Hyun Yoon. In-datacenter performance analysis of a tensor processing unit. In *2017 ACM/IEEE 44th Annual International Symposium on Computer Architecture (ISCA)*, pp. 1–12. IEEE, 2017. (cited on pp. 2 and 3)

Yann LeCun, John S. Denker, and Sara A. Solla. Optimal brain damage. In D. S. Touretzky (ed.), *Advances in Neural Information Processing Systems 2*, pp. 598–605. Morgan-Kaufmann, 1990. URL http://papers.nips.cc/paper/250-optimal-brain-damage.pdf. (cited on p. 1)

Jun Haeng Lee, Sangwon Ha, Saerom Choi, Won-Jo Lee, and Seungwon Lee. Quantization for rapid deployment of deep neural networks, 2018. (cited on p. 3)

Congcong Li. High quality, fast, modular reference implementation of SSD in PyTorch. https://github.com/lufficc/SSD, 2018. (cited on p. 5)

Hao Li, Asim Kadav, Igor Durdanovic, Hanan Samet, and Hans Peter Graf. Pruning filters for efficient convnets. In *International Conference on Learning Representations*, 2017. URL https://openreview.net/forum?id=rJqFGTslg. (cited on p. 1)

Chien-Yu Lin and Bo-Cheng Lai. Supporting compressed-sparse activations and weights on simd-like accelerator for sparse convolutional neural networks. In *2018 23rd Asia and South Pacific Design Automation Conference (ASP-DAC)*, pp. 105–110, Jan 2018. doi: 10.1109/ASPDAC.2018.8297290. (cited on p. 3)

Chunlei Liu, Wenrui Ding, Xin Xia, Yuan Hu, Baochang Zhang, Jianzhuang Liu, Bohan Zhuang, and Guodong Guo. RBCN: Rectified binary convolutional networks for enhancing the performance of 1-bit DCNNs. *arXiv preprint arXiv:1908.07748*, 2019. URL https://arxiv.org/abs/1908.07748. (cited on p. 1)

Wei Liu, Dragomir Anguelov, Dumitru Erhan, Christian Szegedy, Scott Reed, Cheng-Yang Fu, and Alexander C. Berg. Ssd: Single shot multibox detector. In Bastian Leibe, Jiri Matas, Nicu Sebe, and Max Welling (eds.), *Computer Vision – ECCV 2016*, pp. 21–37, Cham, 2016. Springer International Publishing. ISBN 978-3-319-46448-0. (cited on p. 5)

Asit Mishra, Eriko Nurvitadhi, Jeffrey J Cook, and Debbie Marr. Wrpn: Wide reduced-precision networks. *International Conference on Learning Representations*, 2018. URL https://openreview.net/forum?id=B1ZvaaeAZ. (cited on p. 3)

Pavlo Molchanov, Arun Mallya, Stephen Tyree, Iuri Frosio, and Jan Kautz. Importance estimation for neural network pruning. In *The IEEE Conference on Computer Vision and Pattern Recognition (CVPR)*, June 2019. URL http://openaccess.thecvf.com/content_CVPR_2019/html/Molchanov_Importance_Estimation_for_Neural_Network_Pruning_CVPR_2019_paper.html. (cited on p. 1)

Raghid Morcel, Hazem Hajj, Mazen A. R. Saghir, Haitham Akkary, Hassan Artail, Rahul Khanna, and Anil Keshavamurthy. Feathernet: An accelerated convolutional neural network design for resource-constrained fpgas. *ACM Trans. Reconfigurable Technol. Syst.*, 12(2):6:1–6:27, March 2019. ISSN 1936-7406. doi: 10.1145/3306202. URL http://doi.acm.org/10.1145/3306202. (cited on p. 3)

Mohammad Rastegari, Vicente Ordonez, Joseph Redmon, and Ali Farhadi. Xnor-net: Imagenet classification using binary convolutional neural networks. In *European Conference on Computer Vision*, pp. 525–542. Springer, 2016. (cited on p. 5)

Claude E. Shannon. A mathematical theory of communication. *The Bell System Technical Journal*, 27(3):379–423, July 1948. doi: 10.1002/j.1538-7305.1948.tb01338.x. (cited on pp. 2 and 4)

Wojciech Szpankowski. Asymptotic average redundancy of huffman (and shannon-fano) block codes. In *2000 IEEE International Symposium on Information Theory (Cat. No.00CH37060)*, pp. 370–, June 2000. doi: 10.1109/ISIT.2000.866668. (cited on p. 4)

Erwei Wang, James J Davis, Peter YK Cheung, and George A Constantinides. Lutnet: Rethinking inference in fpga soft logic. *arXiv preprint arXiv:1904.00938*, 2019. (cited on p. 3)

Arie Wahyu Wijayanto, Jun Jin Choong, Kaushalya Madhawa, and Tsuyoshi Murata. Towards robust compressed convolutional neural networks. In *2019 IEEE International Conference on Big Data and Smart Computing (BigComp)*, pp. 1–8. IEEE, 2019. (cited on p. 3)

Qingcheng Xiao, Yun Liang, Liqiang Lu, Shengen Yan, and Yu-Wing Tai. Exploring heterogeneous algorithms for accelerating deep convolutional neural networks on fpgas. In *Proceedings of the 54th Annual Design Automation Conference 2017*, DAC '17, pp. 62:1–62:6, New York, NY, USA, 2017. ACM. ISBN 978-1-4503-4927-7. doi: 10.1145/3061639.3062244. URL http://doi.acm.org/10.1145/3061639.3062244. (cited on p. 3)

Yu Xing, Shuang Liang, Lingzhi Sui, Xijie Jia, Jiantao Qiu, Xin Liu, Yushun Wang, Yi Shan, and Yu Wang. Dnnvm: End-to-end compiler leveraging heterogeneous optimizations on fpga-based cnn accelerators. *IEEE Transactions on Computer-Aided Design of Integrated Circuits and Systems*, pp. 1–1, 2019. doi: 10.1109/TCAD.2019.2930577. (cited on p. 3)

Guandao Yang, Tianyi Zhang, Polina Kirichenko, Junwen Bai, Andrew Gordon Wilson, and Christopher De Sa. Swalp: Stochastic weight averaging in low-precision training. *arXiv preprint arXiv:1904.11943*, 2019a. (cited on p. 3)

Jiwei Yang, Xu Shen, Jun Xing, Xinmei Tian, Houqiang Li, Bing Deng, Jianqiang Huang, and Xian-sheng Hua. Quantization networks. In *The IEEE Conference on Computer Vision and Pattern Recognition (CVPR)*, June 2019b. URL http://openaccess.thecvf.com/content_CVPR_2019/html/Yang_Quantization_Networks_CVPR_2019_paper.html. (cited on p. 1)

Tien-Ju Yang, Yu-Hsin Chen, Joel Emer, and Vivienne Sze. A method to estimate the energy consumption of deep neural networks. In *2017 51st Asilomar Conference on Signals, Systems, and Computers*, pp. 1916–1920. IEEE, 2017. (cited on pp. 1, 2, and 3)

Dongqing Zhang, Jiaolong Yang, Dongqiangzi Ye, and Gang Hua. Lq-nets: Learned quantization for highly accurate and compact deep neural networks. In *European Conference on Computer Vision (ECCV)*, 2018. (cited on p. 3)

Yiren Zhao, Xitong Gao, Daniel Bates, Robert Mullins, and Cheng-Zhong Xu. Efficient and effective quantization for sparse dnns. *arXiv preprint arXiv:1903.03046*, 2019. URL http://arxiv.org/abs/1903.03046. (cited on p. 3)

Shuchang Zhou, Zekun Ni, Xinyu Zhou, He Wen, Yuxin Wu, and Yuheng Zou. Dorefa-net: Training low bitwidth convolutional neural networks with low bitwidth gradients. *CoRR*, abs/1606.06160, 2016. URL http://arxiv.org/abs/1606.06160. (cited on p. 5)

A Additional results

We list results of the additional experiments we performed in Tables A.1 and A.2.

Table A.1: Experimental results for ResNet.

Architecture	Batch size	lr	λ	Compute	Memory	Accuracy, %
ResNet-18	96	0.001	0	4	2.050	68.000
			0.05		1.540	67.950
			0.08		1.430	67.860
			0.05	5	1.790	69.490
			0.05		1.750	69.400
			0.1		1.410	69.120
			0.12		1.361	68.900
			0.15		1.280	68.914
			0.18		1.120	68.160
			0.2		1.110	68.300
			0.25		1.040	67.800
			0.3		0.974	67.700
			0	6	3.100	70.000
			0.05		1.930	69.710
			0.08		1.700	69.500
			0.05	7	2.280	69.660
			0	8	5.100	69.900
			0.05		2.460	69.820
			0.08		2.410	69.110
ResNet-34	96	0.001	0.05	8	2.750	73.200
			0.05	6	2.000	73.200
			0.05	5	1.790	73.100
ResNet-50	16	0.0001	0	4	2.500	73.700
	16		0.05		1.720	73.800
	64		0.05		1.78	74.5
	48		0.08		1.67	74.2
	16		0	5	2.950	75.500
	16		0.05		1.920	75.460
	16		0.08		1.700	75.200
	16		0.1		1.600	74.900

Table A.2: Experimental results for MobileNet.

Architecture	Batch size	lr	λ	Compute	Memory	Accuracy, %
MobileNetV2	64	0.0001	0	4	2.200	66.150
	64	0.001	0		2.800	66.200
	64	0.0001	0.05		2.100	66.900
	64	0.001	0.05		2.080	66.400
	64	0.001	0.08		1.830	66.200
	64	0.0001	0.08		1.980	66.450
	64	0.001	0	6	3.900	69.600
	64	0.0001	0		3.700	71.000
	96	0.0001	0.05		2.950	71.500
	32	0.0001	0.08		2.700	70.930
	64	0.0001	0.1		2.700	70.950
	32	0.001	0.15		1.750	64.000
	64	0.0001	0.15		2.600	71.200
	64	0.0001	0.2		2.450	70.700
	64	0.0001	0	8	4.750	71.300
	64	0.0001	0.05		4.150	71.400
	64	0.001	0.08		2.600	70.000
	64	0.0001	0.08		4.120	71.600
	64	0.001	0.1		2.400	69.600
	64	0.0001	0.1		4.100	71.250
	64	0.001	0.15		2.300	68.500
	64	0.001	0.2		2.150	68.000
	64	0.0001	0.2		3.500	71.200
	32	0.0001	0.3		2.900	70.700